Robust Optimization in Nanoparticle Technology: A Proof of Principle by Quantum Dot Growth in a Residence Time Reactor

Jana Dienstbier[a,*], Kevin-Martin Aigner[a], Jan Rolfes[a], Wolfgang Peukert[b], Doris Segets[c], Lukas Pflug[d,e], Frauke Liers[a]

[a] *Friedrich-Alexander-Universität Erlangen-Nürnberg (FAU), Departement of Mathematics, Cauerstraße 11, 91058 Erlangen, Germany*
[b] *Friedrich-Alexander-Universität Erlangen-Nürnberg (FAU), Institute of Particle Technology (LFG), Cauerstraße 4, 91058, Erlangen, Germany*
[c] *Process Technology for Electrochemical Functional Materials, Institute for Combustion and Gas Dynamics – Reactive Fluids (IVG-RF), University of Duisburg-Essen (UDE), Duisburg, Germany*
[d] *Friedrich-Alexander-Universität Erlangen-Nürnberg (FAU), Chair of Applied Mathematics (Continuous Optimization) ,Cauerstraße 11, 91058 Erlangen, Germany*
[e] *Friedrich-Alexander-Universität Erlangen-Nürnberg (FAU), Central Institute for Scientific Computing, Martensstr. 5a, 91058 Erlangen, Germany*

Abstract

Knowledge-based determination of the best-possible experimental setups for nanoparticle design is highly challenging. Additionally, such processes are accompanied by noticeable uncertainties. Therefore, protection against these uncertainties is needed. Robust optimization helps determining such best possible processes. The latter guarantees quality requirements regardless of how the uncertainties, e.g. with regard to variations in raw materials, heat and mass transport characteristics, material properties and (growth) rates, manifest within predefined ranges. To approach this huge task, in this paper we exemplarily model a particle synthesis process with seeded growth by population balance equations and study different growth kinetics. We determine the mean residence time maximizing the product mass subject to a guaranteed yield. Additionally, we hedge against uncertain growth rates and derive an algorithmically tractable reformulation for the robustified problem. We evaluate our approach for seeded growth synthesis of zinc oxide quantum dots and demonstrate computationally that a guaranteed yield is met for all growth rates within previously defined regions. The protection against uncertainties only reduces the maximum amount of product that can be obtained by a negligible margin.

Keywords: particle design, robust optimization, process optimization, reformulation

1. Introduction

The optimal design of nanoparticles consists of many challenging tasks that include the establishment of appropriate experimental setups and processes for fabricating the desired end products. Formulating particle synthesis as a model based optimization problem and solving it via appropriate methods is an important step towards efficient processes that can be implemented in production. For example, robust design in industry must guarantee a certain property, i.e. in case of quantum dots absorption and emission properties as well as quantum yield together with maximum mass yielding economic production. We restrict our approach in this paper to maximize mass - the target depends on the cost functional and thus on the boundary conditions of the system under consideration - within a given target size range, while at the same time quality requirements are met.

Taking nanoparticle synthesis as an example, typically, even at lab-scale the quality of an end product is largely impacted by uncertainties, for example due to unknown thermodynamic parameters such as solubility, flow rates or temperature, to only name a few (see e.g. [1], [2] and [3]). Many of these parameters influence the thermodynamic driving force for particle formation and growth, i.e. supersaturation. Ignoring uncertainties in nanoparticle design, their impact can be so severe that finally the end products are not of the desired quality and need to be discarded completely. In case of new materials and smallest nanoparticles, this aspect is particularly pressing due to the fact that structure-property relationships are often so pronounced that smallest changes in dispersity have a tremendous effect on the product performance (see [4], [5], [6], [7] and [8]). For instance, in case of quantum confined semiconductor nanoparticles, so-called quantum dots, smallest changes in size or a slight increase in dispersity can have a tremendous effect on the position of the band gap or the photoluminscence quantum yield, or both [9].

From an experimental point of view, robust approaches have already been considered which mainly rely on *Taguchi's method* (see [10]) as e.g. in [11]. From a math-

*Corresponding author (**jana.jd.dienstbier@fau.de**)

ematical point of view, robust nanoparticle design has - up to the knowledge of the authors - not been addressed in detail yet. However, mathematical optimization offers the unique possibility to establish optimized processes in such a way that the end products are of the required quality, even under uncertainty and in the worst case scenario. Their influence is intensified when we aim at up-scaling a process from idealized laboratory conditions to industrial production. Then, inaccuracies in set parameters and analytical measurement uncertainties potentiate and the challenge arises to keep the quality requirements even in an up-scaled process.

The mathematical and algorithmic challenges in the approach consist in the development of fast solution algorithms since the corresponding tasks are often modeled as non-linear optimization problems under uncertainty. In order to overcome these challenges, in this work, we use and develop methodologies from the active research field of mathematical optimization under uncertainty, in particular from robust optimization and apply them for the first time to nanoparticle technology.

We demonstrate the value of robust optimization on particle synthesis as this is the very first step in the nanoparticle design chain. In our example, we investigate seeded growth synthesis in reactors considering their residence time distributions, i.e. the distribution of the times the particles remain in the reactor. The goal is to maximize the mass of particles with the quality requirement that the particle size is within a given size range, i.e. maximize the yield for an application-dependent size range. To this end, we consider two different scenarios, reaction-limited and diffusion-limited growth kinetics. A change of only a few degrees in temperature may change the growth kinetics in such a way that the end products are no longer particles within the desired size range. For example, if the growth rate is higher or lower than expected, the particles may either be too large or too small. To overcome these limitations and provide a guaranteed yield even under uncertain growth conditions, we focus on protecting against uncertainties during particle growth.

Since there are several different approaches for optimization with uncertain parameters, in the following we briefly reason why we decided to use robust optimization in this article. One popular approach - especially for handling probabilities - is stochastic optimization, see for example [12]. Stochastic optimization problems contain probabilistic quantities like probability, expected value or higher moments of random variables. It protects against uncertainties with a certain probability and in expectation, see e.g. [13], [12] and [14]. In case of the studied nanoparticle synthesis example we seek to guarantee quality requirements not only with high probability but with certainty. Hence, robust optimization, see [15] is required. Another approach is Semi-infinite Programming (SIP). In SIP, a problem with finitely many variables and infinitely many constraints has to be solved (see [16], [17]). SIP and robust optimization are very closely related, as many robust problems are special SIPs and so the corresponding solution approaches can be used. In our context, we exploit the specific problem structure of the underlying model. Using its quasiconvexity, the robust counterpart allows an algorithmically tractable reformulation that can be solved fast in practice.

In robust optimization, one defines beforehand against which uncertainties protection is sought, which means in our case against deviations in the growth rates. The goal is to determine a process with the highest yield, while at the same time guaranteeing a desired product quality. The robust optimization model developed here is algorithmically tractable and is able to obtain globally optimal solutions. Robustness usually comes with a cost that has to be paid in order to guarantee uncertainty protection, the so-called price of robustness. The *price of robustness* is defined as the percentage of loss compared to the optimal objective value of the nominal, i.e., idealized, problem. For synthesis, it may lead to a reduced yield during the protected process in comparison to what is the maximum achievement at ideal lab conditions.

1.1. Short overview on robust optimization

Suppose we are given a general *nominal optimization problem*, i.e. we ask for a solution vector $x \in \mathbb{R}^n$ that optimizes some objective function $f : \mathbb{R}^n \times \mathbb{R}^m \to \mathbb{R}$ with input parameter $\bar{u} \in \mathbb{R}^m$. In formulas, the optimization problem reads

$$\max_{x \in \mathbb{R}^n} \; f(x, \bar{u}) \tag{1a}$$

$$\text{s.t. } g(x, \bar{u}) \leq 0. \tag{1b}$$

This approach is widely used in process optimization, in the finite-dimensional (see e.g. [18]) but also in the infinite dimensional setting (e.g. time-dependent control, see e.g. [19]).

The situation changes if not all input parameters are known exactly or if their values vary e.g. due to environmental conditions. In robust optimization, we hedge against parameter realizations u that are contained in an a priori defined *uncertainty set* $\mathcal{U} \subset \mathbb{R}^m$. A solution x is called *robust feasible* if it satisfies the constraints regardless of how the uncertainties u manifest themselves within $\mathcal{U}$. A solution x is called *robust optimum* if it attains the best guaranteed objective function value among all robust feasible solutions. The robust optimum solves the corresponding *robust counterpart*

$$\max_{x \in \mathbb{R}^n} \; \min_{u \in \mathcal{U}} \quad f(x, u) \tag{2a}$$

$$\text{s.t.} \quad g(x, u) \leq 0 \quad \forall u \in \mathcal{U}. \tag{2b}$$

Due to the fact that there may be infinitely many constraints and in addition the problem has a max-min structure, it is usually both, computationally and analytically, much harder to solve than the original problem. In general no generic solution approaches exist for such semi-infinite problems.

One way to approach these optimization problems is to restrict $\mathcal{U}$ to a finite set of relevant *scenarios* and approximate the minimum in the optimization by this. This was e.g. in a sophisticated way successfully applied in process optimization by [20]. The main question remaining in this approach is how to choose a relevant set of scenarios which is small enough to be numerically tractable and large enough to get a good approximation of the underlying uncertainty set.

For several relevant classes of optimization problems, it is possible to nevertheless develop efficient solution approaches for the full robust optimization problem. In this case, the robust counterpart is called *algorithmically tractable*. One method to obtain a tractable problem is to reformulate the robust counterpart in a way that the resulting task is a 'standard' finite optimization model that yields correct solutions for the robust counterpart. Along these lines, in Theorem 3.2 we provide such an equivalent reformulation for optimized synthesis processes. In the remainder of this section we briefly illustrate how the setting of a synthesis process fits into the existing literature on robust optimization.

One of the first publications on robust linear problems is [21]. If some duality results hold for the occurring optimization problems, the derivation of an equivalent robust counterpart is often achieved by duality arguments from convex optimization as in [22], and [23], respectively. In the present article such a tractable robust counterpart can be modeled. Geometries for the uncertainty set that are commonly used for a robust protection are polyhedral and ellipsoidal sets. For more details about the possible combinations of constraint function classes together with different geometries, we refer the reader to [24]. Seminal sources for robust optimization include, among others, [25] for discrete problems and [15] for continuous tasks. Key publications about robust protection of more different kinds of optimization problems were published, e.g. on convex optimization, see [26]. We are aware that there are more complex processes in this field, i.e. nonconvex problems or processes with more than one parameter, that has to be optimized. In this case reformulations might no longer be enough to obtain a tractable model. Thus, other tools from robust optimization would be needed. For more general nonconvex robust optimization problems deriving an equivalent reformulation is hardly possible because duality arguments usually do not hold and in general nonconvex problems are difficult. Some recent approaches are for example robust local search methods [27, 28] or decomposition methods like in [29] motivated by outer approximation of semi-infinite problems [30]. Nonlinear robust optimization is surveyed by the authors of [31] to a great extend. The paradigm of robust optimization has been successfully applied in various applications such as logistics [32, 33] or robust energy networks [34, 35].

1.2. Structure of the paper

In Section 2, we introduce the optimized particle synthesis process. To this end, we describe the evolution of the particles within the reactor using an experimentally determined RTD of a microfluidic setup. In Section 3, the approach is extended so that the process is protected against uncertain growth laws in a robust fashion. It is shown that the resulting model can be reformulated to a standard convex optimization problem that can quickly be solved to global optimality by modern available software. Computational results for the different settings, that differ in the growth kinetics (diffusion-limited and reaction-limited) are addressed in Section 4. In our computational evaluations, we show that – for the considered example and settings – robust synthesis is not costly. Indeed, the price of robustness is only a few percents from the maximum yield of idealized lab experiments, whereas in the non-robust setting a significant portion of the end product does not satisfy the quality requirements. We conclude by discussing more generally robust optimization of nanoparticle processes in Section 5.

2. Mathematically optimized synthesis: Sketch of the problem

In this section, we describe the mathematical model for particle synthesis, in particular particle growth.

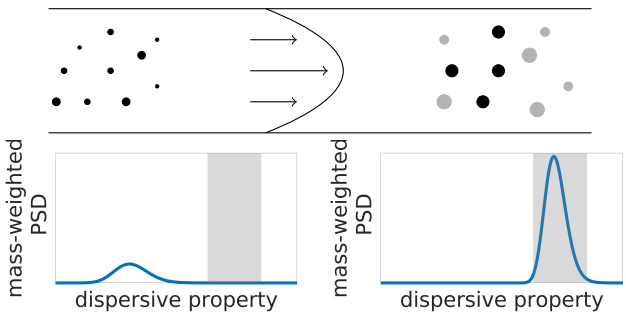

Figure 1: Schematic illustration of a typical continuous growth process. Upper panels: Seeds that grow in a residence time reactor to the target product; lower panels: Initial PSD and product PSD with the target size range highlighted gray

Figure 1 illustrates a typical continuous growth process in particle technology like described in [36], [37] and [38]. In the upper part, we sketch the particle growth in a flow tube. On the left side there are small particles at the start of the process. In the lower part, an initial particle size distribution (PSD) is shown, e.g. after passing a previous nucleation zone. Basically, it describes the distribution of the various particle sizes within the feed. Obviously, the feed consists of small particles that should grow within the flow tube reactor to a set particle size. In the following, we will focus on RTD and assume isothermal conditions. If we assume such conditions, i.e. constant temperature

throughout the whole growth reactor, the RTD defines how long the fluid elements and thus the feed particles stay within the growth zone and thus the dispersity of the end product. Finally, the particles that leave the reactor are grown, as shown on the right side in the upper part. Here, the particles within the "allowed particle size range" are colored in black. However, due to pronounced RTD in a technical process, there will also be particles that are too small or too large. These particles are highlighted in gray in Figure 1. The particle size distribution of the particles within the end product is on the right side below in Figure 1. Thus, the task for robust optimization is to maximize the product mass while it is guaranteed that the yield of our end product meets a certain bound, e.g. 90 %. Due to improve readability, we often simply write size instead of particle size.

2.1. Modeling Particle Synthesis

The basis of modeling the particle growth as part of a synthesis process is the *linear population balance equation* (PBE). In formulas:

$$\partial_t q(t,x) + \partial_x \left(G_g(x) q(t,x)\right) = 0 \qquad \forall t > 0, x > 0, \tag{3a}$$

$$q(0,x) = q_{t0}(x) \quad \forall x > 0, \tag{3b}$$

$$q(t,0) = 0 \qquad \forall t > 0. \tag{3c}$$

Here, $x \in \mathbb{R}_{>0}$ denotes the particle size, $t \in \mathbb{R}_{>0}$ the process time and $G_g : \mathbb{R}_{>0} \to \mathbb{R}_{\geq 0}$ describes the size dependent growth kinetics parametrized by a growth factor $g \in \mathbb{R}$. Furthermore, $q : \mathbb{R}_{>0} \times \mathbb{R}_{\geq 0} \to \mathbb{R}_{\geq 0}$ is the PSD inside the reactor and $q_{t0} : \mathbb{R}_{>0} \to \mathbb{R}_{\geq 0}$ the initial PSD, i.e. the PSD for $t = 0$. The partial derivative with respect to size and time is denoted by ∂_x and ∂_t, respectively. We note that all PSDs considered here are number-weighted in general. Since we will later need two indices, for the sake of clarity we here omit an additional index for the weighting.

In general, growth kinetics depend on the concentrations or equivalently on the solution in a nonlocal way [39, Subsec. 1.2]. The main simplification in the proposed model is, that these concentration effects are neglected. For growth kinetics which depend on the concentration in a multiplicative way (as e.g. modeled in [40, Def. 1.1]), this simplification is "only" a rescaling of the process time. Thus, considering the simplified model still gives insight into how uncertainties in the process conditions will affect the product quality. *We are aware that also supersaturation or solubility influence the growth kinetics and are prone to uncertainty. Thus, in practice it is important to hedge against them as well.* However, then the growth kinetics in formula (3a) itself is a solution of a partial differential equation. Thus, the PBE (3) is in general not solvable analytically. Therefore, we assume that the growth rate fluctuates independently from other parameters within an predefined interval that is predefined in the input (see Section 3). The consideration of supersaturation or solubility will be subject to future work.

Equation (3a) is a partial differential equation modeling the evolution of the particle number density over time supplemented with initial values (3c) for $t = 0$ and zero boundary condition at $x = 0$ stated in (3b). As there is no source term on the right hand side of Equation (3a) and zero boundary condition for $x = 0$ in (3c), no new particles nucleate.

By taking the residence time τ into account, the particles are distributed by the PSD:

$$\bar{q}_{g,\tau}(x) \coloneqq \int_0^\infty E_\tau(t) q_g(t,x) dt, \tag{4}$$

where q_g solves the PBE (3) (for an illustration see final PSD in Figure 1). We recall that these PSDs describe the probability density of particles of one-dimensional size $x \in \mathbb{R}_{>0}$ inside the reactor at process time $t \geq 0$. Further, the probabilistic behavior of the *residence time*, is modeled by the RTD $E_\tau(t)$, with $\tau \in \mathbb{R}_{>0}$ denoting the *mean residence time*.

Since Equation (3a) is a linear balance law, there exists a unique solution for $q_{t0} \in L^1(\mathbb{R}_{>0})$ and $G_g \in L^\infty(\mathbb{R}_{>0})$ locally Lipschitz [39]. The PBE can be solved analytically for a broad class of growth kinetics $G_g(x)$ via the method of characteristics.

As PSDs often exhibit lognormal shape (see e.g. [41]), we consider the initial PSD as being a log-normal distribution. In practice, the seeds are often characterized by their mean particle size and relative standard deviation that can be determined through experiments (see [42] and [43]). Thus, for given mean value $\mu \in \mathbb{R}_{>0}$ and standard deviation $\sigma \in \mathbb{R}_{>0}$ the log-normal q_{t0} considered in the remainder of this article is for all $x > 0$ defined by:

$$q_{t0}(x) = \frac{1}{\sqrt{2\pi \ln\left(\frac{\sigma^2}{\mu^2}+1\right)} x} \cdot \exp\left(- \frac{\left(\ln(x) - \ln\left(\mu \Big/ \sqrt{\left(\frac{\sigma^2}{\mu^2}+1\right)}\right)\right)^2}{2\ln\left(\frac{\sigma^2}{\mu^2}+1\right)} \right) \tag{5}$$

see e.g. [44].

In the following Section 2.1.1, we specify two relevant growth kinetics G_g for which a solution can be obtained analytically: reaction-limited [45] and diffusion-limited growth [46, 45]. In Section 4 we investigate the impact of the specific growth kinetics on the optimal mean residence time τ. Noteworthy, the considerations in the present section are valid for both growth kinetics. For the remainder of this article, this allows us to simply denote the density of the PSD for a fixed growth rate g by q_g without the need to specify g in every instance.

2.1.1. Growth Kinetics

First, we consider reaction-limited growth kinetics, i.e. $G_g(x) = g$, where we assume, that the particles grow constantly over time regardless of their size. We apply the method of characteristics to solve (3) and obtain the unique solution for a given initial datum q_{t0} by:

$$q_g(t,x) = \begin{cases} q_{t0}(x-gt), & \text{if} \quad x - gt > 0, \\ 0, & \text{otherwise.} \end{cases}$$

The second considered growth kinetics in this contribution is diffusion-limited growth, i.e. $G_g(x) = \frac{g}{x}$. In this case the particles grow with decreasing speed for increased sizes. The resulting PBE provides the following solution:

$$q_g(t,x) = \begin{cases} \frac{x}{\sqrt{x^2-2gt}} q_{t0}(\sqrt{x^2-2gt}), & \text{if} \quad x^2 - 2gt > 0, \\ 0, & \text{otherwise.} \end{cases}$$

2.1.2. Residence time in flow reactors

The RTD is dependent on τ, which can be controlled with regard to its mean value by changing the reactor's length for a given flow rate. In a longer reactor, the particles need more time to pass through, i.e. τ is bigger. This results in larger particles at the end of the reactor since the particles have more time to grow. Therefore, by controlling the reactor's length, one controls the mean residence time and with that consequently the resulting particle sizes. Noteworthy, our mathematical framework also lays the foundation for considering a flow-rate dependent change in the shape of the RTD and thus in the width of the resulting PSD as well. In the following, we will consider an RTD fitted to experimental data from [37, Sec. 6, Fig. 10(a)].

The experiments therein were based on a microfluidic setup for continuous nanoparticle synthesis and led to the following RTD:

$$E_\tau(t) = \begin{cases} \frac{1}{\sqrt{2\pi}\sigma_E(t-\tau)} \exp\left(-\frac{(\ln(t-\tau)-\mu_E)^2}{2\sigma_E^2}\right), & t - \tau > 0 \\ 0, & \text{otherwise.} \end{cases} \tag{6}$$

For this RTD, we fitted the parameters μ_E and σ_E to the log-normal distribution on the experimentally determined data points from [37]. In the remainder of this article we focus on this RTD, which is more realistic as it describes real experiments where all fluid elements leave the reactor in a reasonable time frame.

2.2. Optimization of Particle Synthesis

To set up a suitable optimization problem for robust growth during nanoparticle synthesis, we first need to define a range of quantities:

***Total mass*:** Mass of all particles produced through the growth process

***Product mass*:** Mass of all particles that are situated in the target size interval $[x_1, x_2]$, where $0 \leq x_1 < x_2$ are given

Yield : Ratio of product mass to total mass

Loss : Difference of full conversion (1) and yield.

As optimization task, we maximize the product mass while ensuring that a lower bound on the yield $P_{\min} \in [0,1]$ is satisfied. The latter is given, e.g., by quality and economical requirements from industry like a certain yield that must be produced to make the process economically feasible. Among the different variables that could be optimized, e.g. temperature, flow rate or reactor dimensions, we concentrate on the mean residence time τ. The reason for our choice is that we can realize an optimal τ by building a reactor of the corresponding length or adjusting its flow speed accordingly. As we consider the mass of the synthesized particles as yield, we multiply $\bar{q}_{g,\tau}(x)$ with x^3 and neglect constants as the optimum solution of the optimization problem is invariant of. We obtain the following objective function:

$$J_g(x_1, x_2, \tau) = \int_{x_1}^{x_2} x^3 \int_0^\infty E_\tau(t) q_g(x,t) dt dx.$$

The objective is to find the optimal mean residence time τ such that the mass of particles that reach the end of the reactor with a size $x \in [x_1, x_2]$ is maximized, i.e. we maximize $J_g(x_1, x_2, \tau)$ (which is proportional to the aimed mass) with respect to $\tau > 0$.
At this point it must be mentioned that mass is acting here as a showcase example. We decided on mass, since producing as much as possible has a major impact on the profit and of course quality requirements have to be met since the end product has to satisfy the needs of possible costumers. However, we are aware, that in a real-world application (or business case, actually) the cost functional would contain additional factors such as the width of the particle size distribution, temperature or time, etc. For the proof of principle of robust optimization in particle technology that we show here, we use this comparatively straight-forward showcase. This setting is already highly challenging from an application point of view, and the benefits of robust optimization are clearly visible.

Since we assume that there is no post-synthetic classification step, although approaches like chromatography are coming in reach like described in [47] and [48], the yield at the end of the reactor can either be taken or rejected as a whole but not partially. Thus, we demand that a purity of at least $P_{\min}$ has to be met to guarantee a certain share of particles within the right size. Since the total mass can be denoted by $J_g(0, \infty, \tau)$, we obtain as a yield constraint:

$$\frac{J_g(x_1, x_2, \tau)}{J_g(0, \infty, \tau)} \geq P_{\min}.$$

Thus, we formulate the problem for optimizing the synthesis process as:

$$\max_{\tau>0} \; J_g(x_1, x_2, \tau), \tag{7a}$$

$$\text{s.t. } \frac{J_g(x_1, x_2, \tau)}{J_g(0, \infty, \tau)} \geq P_{\min}. \tag{7b}$$

Problem (7) is a continuous nonlinear optimization problem (NLP). Commonly, one determines a first-order optimal solution with the help of local search methods like interior point methods [49]. A detailed overview of numerical methods for NLPs can be found in [50]. Such local optimization solvers typically only determine locally but not necessarily globally optimal solutions. Although the computational effort is relatively low, convergence of local solvers is in general not guaranteed and depends heavily on the chosen initial value. In addition, local solutions can be much worse, when compared to the global solution. An additional difficulty is posed by the integration terms. Many commercial solvers are not compatible with these expressions.

We thus analyze the structure of problem (7) in order to develop an efficient solution approach. By-eye inspection, it turns out that in the intervals of τ and g considered in Section 4, the first derivative of the functions of product mass as well as the yield has at most one change of sign. This property is called *quasiconcavity* that we define next.

Definition 2.1 (Quasiconcavity)**.** *A set $\mathcal{S} \subset \mathbb{R}^n$ is called convex if for $y, z \in \mathcal{S}$ and $\lambda \in [0,1]$: $\lambda y + (1-\lambda) z \in \mathcal{S}$ holds. A function $k : \mathcal{S} \subset \mathbb{R}^n \to \mathbb{R}$ defined on a convex subset $\mathcal{S} \subset \mathbb{R}^n$ is called quasiconcave if for every $y, z \in \mathcal{S}$ and $\lambda \in [0,1]$ the inequality $k(\lambda y + (1-\lambda) z) \geq \min\{k(y), k(z)\}$ holds.*

Density functions of unimodal distributions are quasiconcave. Additionally, it can be assumed that quasiconcave initial PSDs such as log-normal distributions lead to quasiconcave PSDs over time as long as neither nucleation nor agglomeration is involved. This indicates that the functions in (7) are quasiconcave. We formalize this in the following assumption.

Assumption 2.2 (Quasiconcave objective functional and constraint)**.** *The functions $J_g(x_1, x_2, \tau)$ and $\frac{J_g(x_1, x_2, \tau)}{J_g(0, \infty, \tau)}$ are quasiconcave in τ for fixed $0 \leq x_1 < x_2$.*

This implies that the smallest objective value is attained at the boundaries of the feasible set, if the latter is convex. This allows us to establish the convexity of the feasible set.

Lemma 2.3. *Under Assumption 2.2, the feasible set $\mathcal{S} := \left\{\tau > 0 : \frac{J_g(x_1, x_2, \tau)}{J_g(0, \infty, \tau)} \geq P_{min}\right\}$ is convex.*

Proof. Denote the constraint function as $h(\tau) := \frac{J_g(x_1, x_2, \tau)}{J_g(0, \infty, \tau)}$. For $\tau_1, \tau_2 \in \mathcal{S}$ with $\tau_1 \neq \tau_2$, due to quasiconcavity $h(\lambda \tau_1 + (1-\lambda)\tau_2) \geq \min\{h(\tau_1), h(\tau_2)\} \geq P_{\min}$ holds for every $\lambda \in [0,1]$. As this is true for all values $\tau_1, \tau_2 \in \mathcal{S}$ the claim is proven. □

The quasiconcavity of the objective function and the convexity of the feasible set establish that, like in a classical convex optimization problem, every local solution of (7) is also globally optimal like shown in Section 3. Thus, Problem (7) can be solved to global optimality with available standard solvers for NLPs, e.g. `IPOPT` [51], `CONOPT` [52] or `matlab` [53] internal `FMINCON`.

3. Robust Optimization of Particle Synthesis under uncertainty

So far, we only discussed nominal optimization of particle synthesis. In this section we extend our model by hedging against uncertainties in the growth kinetics.

For specifying the uncertainty set, let the nominal value for the growth rate in idealized lab conditions be given by $g_0 > 0$. Since the reactor temperature could slightly differ during the process, the uncertainty set should mimic slower or faster growth rates. We define a relative error by a fraction $\Delta \in [0,1]$ as variations of g against which we want to hedge against and define the uncertainty set as the interval $[g_0 - \Delta g_0, g_0 + \Delta g_0]$.

A robust optimum solution τ^* is feasible for every realization of g within the uncertainty set, i.e., $g \in [g_0 - \Delta g_0, g_0 + \Delta g_0]$ and maximizes the guaranteed product mass. In formulas, the robust counterpart is:

$$\max_{\tau>0} \min_{g \in [g_0 - \Delta g_0, g_0 + \Delta g_0]} \; J_g(x_1, x_2, \tau) \tag{8a}$$

$$\text{s.t. } \frac{J_g(x_1, x_2, \tau)}{J_g(0, \infty, \tau)} \geq P_{\min} \tag{8b}$$

$$\text{for all } g \in [g_0 - \Delta g_0, g_0 + \Delta g_0].$$

Problem (8) is a robust Nonlinear Program with nonlinear objective and semi-infinite constraints due to the for-all constraint. For this problem class, no general solution approach exists.

In order to nevertheless be able to solve it efficiently, we exploit the problem structure as follows. By numerical evidence, the product mass as well as the yield are quasiconcave not only in τ but also quasiconcave in g within the considered intervals. We formulate the quasiconcavity with respect to g as follows:

Assumption 3.1. *The functions $J_g(x_1, x_2, \tau)$ and $\frac{J_g(x_1, x_2, \tau)}{J_g(0, \infty, \tau)}$ are quasiconcave in g for all fixed $0 \leq x_1 < x_2$ and $\tau > 0$.*

Under Assumption 2.2, the minimum of $J(x_1, x_2, \tau)$ is attained either at $g = g_0 - \Delta g_0$ or at $g = g_0 + \Delta g_0$. Furthermore, due to quasiconcavity, if a solution to Problem (7) is feasible for the largest and for the smallest growth rate, it is feasible for all growth rates in between. This leads to the following convex reformulation of (7) that is solvable efficiently by available software:

Theorem 3.2. *Under Assumptions 2.2 and 3.1, Problem (8) can be reformulated as the following convex optimization model:*

$$\max_{\tau,z>0} \quad z \tag{9a}$$
$$s.t. \quad J_{g_0-\Delta g_0}(x_1,x_2,\tau) \geq z, \tag{9b}$$
$$J_{g_0+\Delta g_0}(x_1,x_2,\tau) \geq z, \tag{9c}$$
$$\frac{J_{g_0-\Delta g_0}(x_1,x_2,\tau)}{J_{g_0-\Delta g_0}(0,\infty,\tau)} \geq P_{min}, \tag{9d}$$
$$\frac{J_{g_0+\Delta g_0}(x_1,x_2,\tau)}{J_{g_0+\Delta g_0}(0,\infty,\tau)} \geq P_{min}. \tag{9e}$$

Proof. First, we rewrite the objective (8a). Due to Assumption 3.1, the minimum of $J(x_1,x_2,\tau)$ for each τ is either attained at $g = g_0 + \Delta g_0$ or at $g = g_0 + \Delta g_0$. Thus, we introduce an additional variable z with $z \leq J_{g_0-\Delta g_0}(x_1,x_2,\tau)$ and $z \leq J_{g_0+\Delta g_0}(x_1,x_2,\tau)$. A maximal z satisfying these constraints therefore correctly attains the minimum of the objectives evaluated at the limits of the considered g interval. Next, we reformulate the yield constraint. Since:

$$\frac{J_g(x_1,x_2,\tau)}{J_g(0,\infty,\tau)} \geq P_{\min} \quad \forall g \in [g_0-\Delta g_0, g_0+\Delta g_0]$$
$$\Leftrightarrow \quad \min_{g\in[g_0-\Delta g_0,g_0+\Delta g_0]} \frac{J_g(x_1,x_2,\tau)}{J_g(0,\infty,\tau)} \geq P_{\min}.$$

Consequently, we write Problem (8) as:

$$\max_{\tau,z>0} \quad z \tag{10a}$$
$$\text{s.t.} \quad J_{g_0-\Delta g_0}(x_1,x_2,\tau) \geq z, \tag{10b}$$
$$J_{g_0+\Delta g_0}(x_1,x_2,\tau) \geq z, \tag{10c}$$
$$\min_{g\in[g_0-\Delta g_0,g_0+\Delta g_0]} \frac{J_g(x_1,x_2,\tau)}{J_g(0,\infty,\tau)} \geq P_{\min}. \tag{10d}$$

For reformulating (8b), we use Assumption 3.1 and obtain that $\frac{J_g(x_1,x_2,\tau)}{J_g(0,\infty,\tau)}$ attains its minimum at $g = g_0 - \Delta g_0$ or at $g = g_0 + \Delta g_0$. Consequently, this leads to the equivalence:

$$\min_{g\in[g_0-\Delta g_0,g_0+\Delta g_0]} \frac{J_g(x_1,x_2,\tau)}{J_g(0,\infty,\tau)} \geq P_{\min}$$
$$\Leftrightarrow \quad \frac{J_g(x_1,x_2,\tau)}{J_g(0,\infty,\tau)} \geq P_{\min} \text{ for } g = g_0 \pm \Delta g_0.$$

Thus, Problem (9) is a reformulation of Problem (8).

It remains to show that every locally optimal solution is also globally optimal. Assumption 2.2 allows to apply Lemma 2.3 and obtain that the feasible set of (9) is convex. Since the new objective is linear and thus concave, we immediately obtain that every locally optimal solution of Problem (9) is also globally optimal. □

The main benefit of Theorem 3.2 is that the reformulated problem is a standard convex optimization problem for which the same standard solvers as for Problem (7) determine global optima.

4. Computational Results

In this section we present numerical results for the robust process optimization of ZnO nanoparticle growth. Based on [37], we assume as initial PSD (seed) q_{t0} a log-normal distribution with mean size $\tilde{\mu} = 1.8$ nm and a relative standard deviation of $\tilde{\sigma} = 10$ %. Through (5), as shown in Figure 1, this leads to an initial PSD of:

$$q_{t0}(x) = \frac{1}{\sqrt{0.02\pi}x} \exp\left(-\frac{(\ln(x)-0.58)^2}{0.02}\right).$$

This PSD is used for the initial condition (3b) in (3). We demonstrate our approach in an exemplary manner for a target particle size interval $[x_1,x_2]$, where $x_1 = 3.0 - 0.3$ nm and $x_2 = 3.0 + 0.3$ nm. These particles shall grow with a nominal growth rate g_0 of 0.2 $\frac{\text{nm}}{\text{min}}$. For the deviation in the growth rate we chose 10 % as this indicates a transition to so-called 'narrow' PSDs [43], [54] and [1]. Therefore, the uncertainty set is chosen as $g \in [0.18 \frac{\text{nm}}{\text{min}}, 0.22 \frac{\text{nm}}{\text{min}}]$.

We solve Problem (7) and Problem (9) for the two growth kinetics defined in Section 2. Since the choice of the growth kinetics has a huge impact on the PSD at the reactor's end, not every yield can be reached with every configuration, thus $P_{\min}$ has to be differently for different growth kinetics. We always set it to the highest value for which it was possible to find a robust feasible solution. Interestingly, we will see later that from all chosen models, we can robustly guarantee the highest yield for the physically most realistic modeling of the RTD and growth kinetics.

First, we use the measured RTD from [37], see Section 4.1, with μ_E=0.8 and σ_E=0.25 and reaction-limited growth and obtain an optimal solution for a minimal yield of 75 %. The second configuration is the more realistic one for small particles, consisting of the measured RTD and diffusion-limited growth (Section 4.2). The robust counterpart for that configuration can be solved for a minimal yield of 90 %. If the problem is feasible for such a large $P_{\min}$, high quality regarding the desired particle size of the total mass can be guaranteed.

We solve Problem (7) and Problem (9) with a standard notebook within seconds. For optimizing the nonlinear optimization problems, we use the `Matlab` internal optimization toolbox `fmincon` [53]. The evaluation of occurring integral expressions is executed with the function `int`.

We further evaluate the robust solutions by computing their price of robustness, that we recall from Section 1. Let z_{nom} be the optimal value of Problem (1) and z_{rob} the optimal value for the robust Problem (2). The price of robustness is determined as:

$$\frac{z_{\text{nom}} - z_{\text{rob}}}{z_{\text{nom}}}. \tag{11}$$

If this value is limited, the process can be implemented efficiently in practice. If its value cannot be accepted in

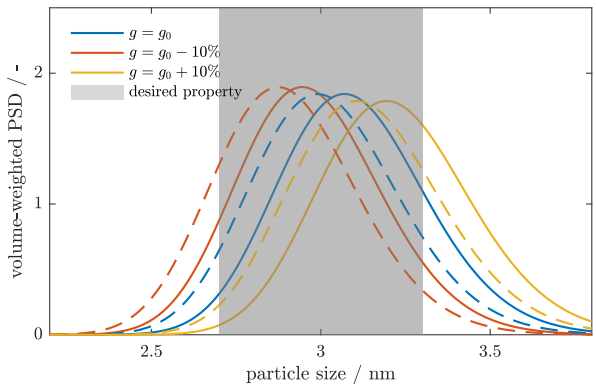

Figure 2: PSDs at the reactor outlet derived for different growth rates and the nominal (solid curves) and the robust (dashed curves) optimal τ. The areas under the curves are proportional to the respective masses.

.

practice, the question arises which uncertainties largely influence it, and whether it can be reduced, e.g., by incorporating additional measurements.

4.1. Results for Reaction-Limited Growth Kinetics

In this setting, the RTD $E_\tau(t)$ is log-normally distributed with μ_E and σ_E fitted to the data from [37]. As growth kinetics we consider reaction-limited growth $G_g(x) = g$ and derive q_g by inserting this growth rate to the linear PBE (3) with the above initial PSD q_{t0} as described in Section 2.1.1.

In this setting, there is no robust solution that guarantees a yield $P_{\min}$, i.e. a ratio of particles in the desired size range, of 80 %. However, it is $\tau_{\text{nom}} = 6.28$ and $\tau_{\text{rob}} = 5.88$ for $P_{\min} = 0.75$. From (Figure 2) it becomes clear that the density distributions do not have significant tails. As the parabolas are still broader than the desired size interval, no yield greater or equal to 80 % could be reached for any realization of growth rates $g \in \{0.18\ \frac{\text{nm}}{\text{min}}, 0.2\ \frac{\text{nm}}{\text{min}}, 0.22\ \frac{\text{nm}}{\text{min}}\}$. One observes that with increasing values of g the parabola is shifted to the right. Thus, the nominal optimal total mass with $g = 0.22\ \frac{\text{nm}}{\text{min}}$ again becomes infeasible. The graphs of the densities with τ_{rob} are shifted to the left and flattened, when compared to τ_{nom}. We determined the yields for $g_0 - \Delta g_0$, g_0 and $g_0 + \Delta g_0$ with τ_{nom} and τ_{rob} and summarized them in Table 1.

Table 1: Yield for three different growth rates.

\ growth rate	$g_0 - \Delta g_0$	g_0	$g_0 + \Delta g_0$
yield, nominal	0.84	0.80	0.64
yield, robust	0.79	0.83	0.75

From the results shown in Table 1, the benefit from robust optimization is clearly visible. Although the nominal yield for $g_0 - \Delta g_0$ is slightly larger than that for the robust optimal τ, for $g_0 + \Delta g_0$ the yield requirement is not satisfied. This means that if the uncertain growth rate

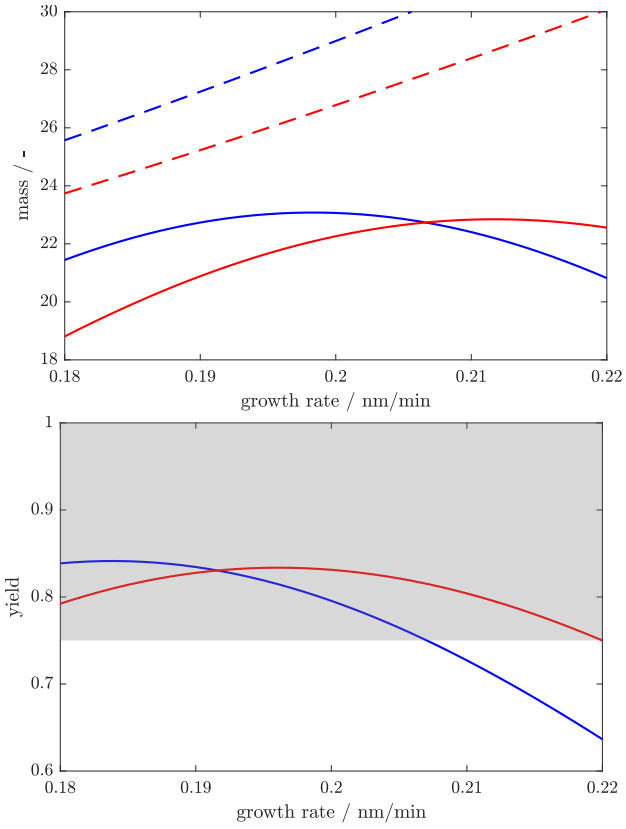

Figure 3: Upper panel: Total mass (dashed line) and product mass (solid line) in dependence of g for τ_{nom} (blue) and τ_{rob} (red). Lower panel: Yields in dependence of g for τ_{nom} (blue line) and τ_{rob} (red line).

manifests itself as $g_0 + \Delta g_0$, the *whole* end product has to be discarded completely, whereas it still can be used when the robust solution is implemented. In addition, it turns out and as will be described in more detail in the following, that this protection is not costly. Indeed, the price of robustness (11) is - at least in the given case - low and not more than about 3.5 %.

Figure 3 illustrates the product mass, the total mass and the yield with respect to the growth rate. The graph of the optimal product mass obtained in the nominal setting is a parabola with a maximum at g_0, whereas in the robust case the maximum is attained between g_0 and $g_0 + \Delta g$ and remains quite high. The graph of the yields is also a parabola. However, as ensured by the robust model (9), the robust yield remains feasible for all considered growth rates, whereas the nominal yield falls below 0.75 at a certain point of the interval $[0.205\ \frac{\text{nm}}{\text{min}}, 0.206\ \frac{\text{nm}}{\text{min}}]$. Using the robust mean residence time τ_{rob}, a yield of 75 % is ensured regardless of how the growth rate manifests itself within the uncertainty interval. Compared to an idealized process under lab conditions the robust process, i.e. with τ_{rob}, produces 3.5 % less product mass. From Figure 3 we observe that for $\tau = \tau_{\text{nom}}$ and a growth rate larger than $0.207\ \frac{\text{nm}}{\text{min}}$, the yield falls below $P_{\min}$. Then, the total mass needs to be disposed completely. If we assume a uniformly dis-

tributed uncertainty in g, we would produce a useless end product in about 32.5 % of all processes. The robust solution avoids such violation of quality requirements, only by the low cost of loosing 3.5 % in mass. This already shows how RO and knowledge on the price of robustness help estimating the feasibility (or risks) of certain products and the related processes.
In the following Section 4.2 reaction-limited growth will be replaced by the, at least for fast precipitating nanoparticles, more realistic diffusion-limited growth (see [2] and [55]). However, the exact particle formation mechanism of quantum dots is still not unraveled and rather likely might become more complex than expected (see [56], [57] and [58]) .

4.2. Results for Diffusion-Limited Growth Kinetics

In this subsection we derive $\bar{q}$ by using the RTD (6) determined with data from [37] and the diffusion-limited growth kinetics $G_g(x) = \frac{g}{x}$, see Section 2.1.1. Both, the PSD at the start and the RTD are assumed to follow log-normal distributions with the same parameters as in the last section. We solved the nominal problem (7) and the robust problem (9) with a guaranteed yield of $P_{\min} = 0.9$. For a higher yield the robust problem is infeasible which implies that regardless of how the growth rate manifests itself within the uncertainty set, it is not possible to determine a mean residence time so that quality requirements of the end product are met.
With a guaranteed yield of 90 %, we obtained $\tau_{\text{nom}} = 16.04$ for the nominal and $\tau_{\text{rob}} = 14.97$ for the robust problem. In Figure 4, the volume PSDs $x^3\bar{q}_{\tau,g}(x)$ for $g \in \{g_0 - \Delta g_0, g_0, g_0 + \Delta g_0\}$ and $\tau \in \{\tau_{\text{nom}}, \tau_{\text{rob}}\}$ are shown.

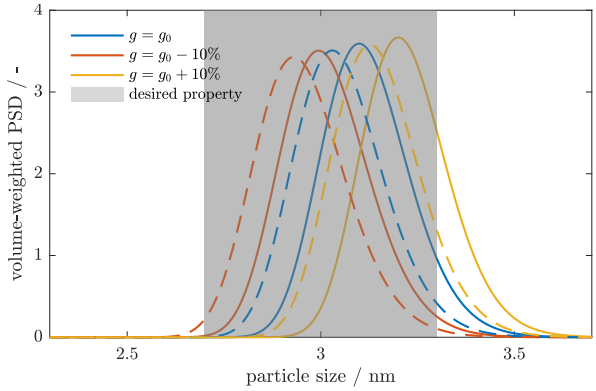

Figure 4: PSDs at the reactor outlet derived for different growth rates and the nominal (solid curves) and the robust (dashed curves) optimal τ. The areas under the curves are proportional to the respective masses.

.

As in Section 4.1, the densities at the reactor outlet have one maximum but in the current model the width of the distribution is much smaller and thus clearly more favorable with regard to typical applications of quantum dots like light emitting diodes with high emission (compare steepness and peak height with Figure 2). With regard to optimization, narrow distributions are key to guarantee a high yield since more volume is contained in the desired size interval $[x_1, x_2]$.
With increasing growth rate the peak shifts to the right and the whole graph is stretched. We observe that on the one hand for nominal optimal τ the maximum value is larger than for robust optimal τ. On the other hand if $g = g_0 + \Delta g_0 = 0.22\ \frac{\text{nm}}{\text{min}}$, the graph exceeds x_2 widely and the yield requirement can not be satisfied anymore. Contrarily, in the robust optimal case one observes again, that all three graphs mostly lie within the desired size range. Compared to Section 4.1, we consequently expect the same pattern of values except for a higher yield. Table 2 confirms this expectation.

Table 2: Yield for three different growth rates.

\ growth rate	$g_0 - \Delta g_0$	g_0	$g_0 + \Delta g_0$
yield nominal	0.98	0.93	0.77
yield robust	0.99	0.97	0.90

If the particles grow at a rate of $g_0 + \Delta g_0$, the nominal optimal τ violates the requirements since $0.77 < 0.9$, whereas the robust optimal τ meets the requirements for all considered growth rates.
As in the previous sections, we illustrate the product mass and the total mass as well as the yield with respect to g in Figure 5. The nominal product mass increases slowly for $g < 0.2\ \frac{\text{nm}}{\text{min}}$ and then decreases fast, whereas the robust total mass increases fast for $g < 0.22\ \frac{\text{nm}}{\text{min}}$ and then decreases slowly. The nominal yield is a quickly decreasing function and falls below 0.9 in the interval $[0.206\ \frac{\text{nm}}{\text{min}}, 0.22\ \frac{\text{nm}}{\text{min}}]$. The robust yield is decreasing much slower and remains feasible.

As in Section 4.1, we have to pay a price of robustness (11). However this time, we only have to pay 2.3 %. From Figure 5 we observe that for $\tau = \tau_{\text{nom}}$ and a growth rate $> 0.206\ \frac{\text{nm}}{\text{min}}$ the corresponding total mass has to be disposed. If we again assume a uniformly distributed uncertainty in g, we have to dispose the end product in about 35.0 % of the processes. Eventually, we suffer an even smaller loss of 2.3 % as price of robustness compared to the higher share of 35.0 % of the synthesis processes that become infeasible for the nominal optimal τ.

4.3. Properties of the robustification

In general, for optimizing the product mass, large particles within the desired size range are preferred over small ones, which corresponds to larger values of τ. However, we noticed that the yield for the nominal optimal product mass with respect to g_0 is strictly greater than $P_{\min}$. Thus, τ could be increased without obtaining an infeasible solution for the nominal growth rate g_0. But surprisingly this leads to a decrease in the objective value instead of a further increase. The reason for this effect is the following: By increasing τ, the graph of the density shifts to the right

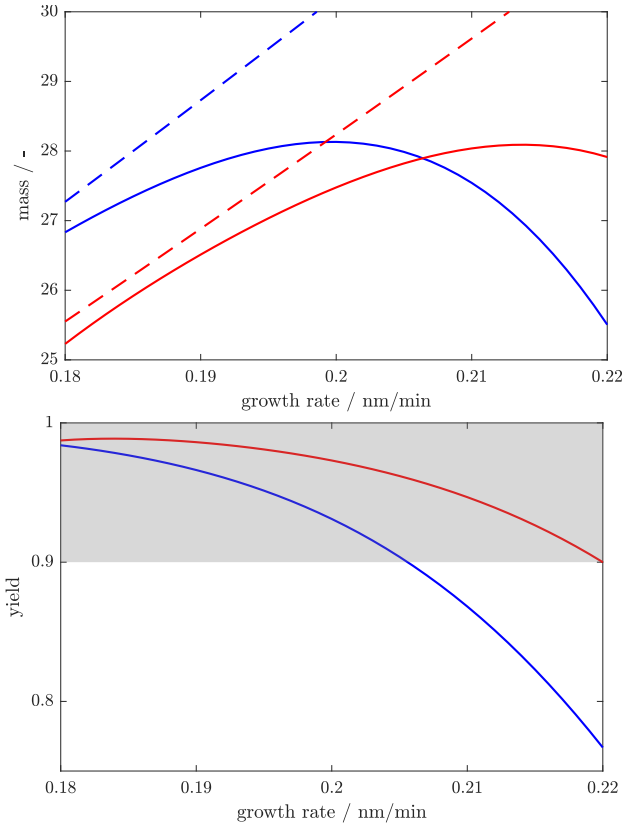

Figure 5: Upper panel: Total mass (dashed line) and product mass (solid line) in dependence of g for τ_{nom} (blue) and τ_{rob} (red). Lower panel: Yields in dependence of g for τ_{nom} (blue line) and τ_{rob} (red line).

and the particles grow larger, but also a significant share of the particles grows too large. Thus, the best value for τ is given by a trade-off between increasing the product mass through larger particles and loosing product mass if the particles grow too large. Hence, the ideal location of the PSD for maximizing the product mass does not necessarily coincide with a location that satisfies the yield constraint exactly.

In the robust case we observe this effect only for reaction-limited growth. In case of diffusion-limited growth, the product mass further increases for growing τ but is limited by the yield constraint which is fulfilled with equality for the worst-case scenario $g = g_0 + \Delta g_0$.

Let us now elaborate on the feasibility of the solutions in both models. The nominal optimal graph of the mass-weighted PSD $x^3 \bar{q}_{g_0,\tau_{nom}}$ shifts to the right with growing g. Thus, setting $g = g_0 + \Delta g_0 = 0.22 \frac{\text{nm}}{\text{min}}$ pushes the main volume below the graph out of the desired size interval $[x_1, x_2]$ and leads to a violation of the yield constraint (see e.g. Figure 4). If we set $g = g_0 - \Delta g_0 = 0.18 \frac{\text{nm}}{\text{min}}$, the graph shifts to the left, remains inside of $[x_1, x_2]$ and thus is still feasible.

As robustification aims to guarantee feasibility also for the considered interval limits $g_0 + \Delta g_0$, the graphs of the densities are shifted to the left and therefore, the robust optimal τ is always smaller than the nominal optimal one, i.e. $\tau_{\text{rob}} < \tau_{\text{nom}}$. This indicates that reactors should be built shorter than under idealized lab conditions ensuring that the yield constraint is met for every uncertain $g \in [g_0 - \Delta g_0, g_0 + \Delta g_0]$.

In summary, it can be said that the nominal idealized model is feasible for $g \in [g_0 - \Delta g_0, g_0]$ but gets infeasible above a certain $g \in [g_0, g_0 + \Delta g_0]$. In contrast, robust optimal solutions are feasible for every $g \in [g_0 - \Delta g_0, g_0 + \Delta g_0]$ as was illustrated in Figure 3 and Figure 5.

The price of robustness is about 3.5 % in Subsection 4.1 and 2.3 % in Subsection 4.2. Since in Subsection 4.1 we would dispose 32.5 % and in Subsection 4.2 35.0 % of our outcomes in the nominal case. Thus, RO allows us - at least in the considered (simplified) examples - to protect our experimental design against uncertainties at a low cost of at most 3.5 %. Furthermore, robust optimization approaches as outlined here can be developed for a wide range of problems and processes in nanoparticle technology.

5. Conclusions and Outlook

In this work, we have observed that robust protection against uncertainties is very valuable for synthesis in reactors modeled by RTDs. In particular, we considered a synthesis process, whose initial, time-dependent PSD is derived from a PBE with different growth kinetics. To describe the behavior of the particle inside the reactor, we fit the RTD to measured values from [37]. Consequently, the particle sizes at the end of the reactor are distributed with the convolution of the above PSD and RTD over time.

For these different growth kinetics and the fitted RTD we established a mathematical optimization problem that computes the optimal mean residence time maximizing the product mass of the process, while guaranteeing a given minimal yield of the end product. We then extended this optimization problem to be able to deal with uncertainties in the growth rate. Here, we applied methods from robust optimization to compute an optimal mean residence time – a residence time that maximizes the product mass for the worst realization of uncertainty and simultaneously ensures that the yield constraints are met for every realization of uncertainty within the considered uncertainty set.

Subsequently, we demonstrate this approach at the example of ZnO nanoparticle synthesis and a uncertainty of 10 % in the growth rate. For example, one observes that if the process is modeled by diffusion-limited growth behavior combined with the RTD stemming from [37], our optimization can guarantee a purity of 90 % of the resulting yield. Furthermore, the loss of 2.3 % of the mass in product compared to a model that does not protect against uncertainties and thus potentially disposes entire charges of end product, is acceptable.

Along these lines, we want to stress possible extensions of our approach. Although we only considered the case of uncertain growth and a simplified cost function (in terms

of application), we suppose that the method could also be beneficial for uncertainties caused by temperature, inaccuracies in the flow rate or even pulsation, or measurement errors during derivation of material properties. Furthermore, also in other processes in particle science and technology, that are strongly dependent on the RTD such as chromatography, parameters are varying and uncertainties have a huge impact on the outcome. Thus, the concept of robust protection might be key to establish a more general methodology to deal with uncertainties in the context of nanoparticle design, for example also in particle separation and characterization, or in their suitable combination. We believe that in particular in the context of disperse systems, robust optimization will play a key role in bringing new materials and technologies into the market.

In future work, the nonlinearity of the PBE (3a) - the nonlocal dependency of the growth rate on the solution due to conservation of mass, see e.g. [40, Def. 1.1.] - needs to be taken into account. By this, uncertainties in e.g. temperature and solubility can directly be considered. Further, uncertainties in the initial PSD is of great interest.

Acknowledgment
This paper has been founded by the Deutsche Forschungsgemeinschaft (DFG, German Research Foundation) - Project-ID 416229255 - SFB 1411.

References

[1] A. M. Salaheldin, J. Walter, P. Herre, I. Levchuk, Y. Jabbari, J. M. Kolle, C. J. Brabec, W. Peukert, D. Segets, Automated synthesis of quantum dot nanocrystals by hot injection: Mixing induced self-focusing, Chemical Engineering Journal 320 (2017) 232–243.

[2] J. Gradl, H.-C. Schwarzer, F. Schwertfirm, M. Manhart, W. Peukert, Precipitation of nanoparticles in a t-mixer: coupling the particle population dynamics with hydrodynamics through direct numerical simulation, Chemical Engineering and Processing: Process Intensification 45 (2006) 908–916.

[3] L. Metzger, M. Kind, The influence of mixing on fast precipitation processes–a coupled 3d cfd-pbe approach using the direct quadrature method of moments (dqmom), Chemical Engineering Science 169 (2017) 284–298.

[4] A. P. Alivisatos, Semiconductor clusters, nanocrystals, and quantum dots, science 271 (1996) 933–937.

[5] D. V. Talapin, A. L. Rogach, A. Kornowski, M. Haase, H. Weller, Highly luminescent monodisperse cdse and cdse/zns nanocrystals synthesized in a hexadecylamine- trioctylphosphine oxide- trioctylphospine mixture, Nano letters 1 (2001) 207–211.

[6] O. I. Micic, C. J. Curtis, K. M. Jones, J. R. Sprague, A. J. Nozik, Synthesis and characterization of inp quantum dots, The Journal of Physical Chemistry 98 (1994) 4966–4969.

[7] C. Burda, X. Chen, R. Narayanan, M. A. El-Sayed, Chemistry and properties of nanocrystals of different shapes, Chemical reviews 105 (2005) 1025–1102.

[8] R. Viswanatha, S. Sapra, B. Satpati, P. Satyam, B. Dev, D. Sarma, Understanding the quantum size effects in zno nanocrystals, Journal of Materials Chemistry 14 (2004) 661–668.

[9] M. L. Mastronardi, F. Maier-Flaig, D. Faulkner, E. J. Henderson, C. Kübel, U. Lemmer, G. A. Ozin, Size-dependent absolute quantum yields for size-separated colloidally-stable silicon nanocrystals, Nano letters 12 (2012) 337–342.

[10] K.-L. Tsui, An overview of taguchi method and newly developed statistical methods for robust design, Iie Transactions 24 (1992) 44–57.

[11] K. Do Kim, D. W. Choi, Y.-H. Choa, H. T. Kim, Optimization of parameters for the synthesis of zinc oxide nanoparticles by taguchi robust design method, Colloids and Surfaces A: Physicochemical and Engineering Aspects 311 (2007) 170–173.

[12] J. Birge, F. Louveaux, Introduction to Stochastic Programming, Springer Series in Operations Research and Financial Engineering, Springer New York, 2006.

[13] A. Prekopa, B. Vizvari, T. Badics, Programming under probabilistic constraint with discrete random variable, in: New trends in mathematical programming, Springer, 1998, pp. 235–255.

[14] A. Ruszczyński, A. Shapiro, Stochastic Programming, Handbook in Operations Research and Management Science, 2003.

[15] A. Ben-Tal, L. El Ghaoui, A. Nemirovski, Robust Optimization, Princeton Series in Applied Mathematics, Princeton University Press, 2009.

[16] H. Djelassi, A. Mitsos, O. Stein, Recent advances in nonconvex semi-infinite programming: Applications and algorithms, Optimization Online (2021). Preprint ID 2021-02-8258.

[17] R. Hettich, K. O. Kortanek, Semi-infinite programming: theory, methods, and applications, SIAM review 35 (1993) 380–429.

[18] M. P. Elsner, G. Ziomek, A. Seidel-Morgenstern, Simultaneous preferential crystallization in a coupled, batch operation mode—part i: Theoretical analysis and optimization, Chemical engineering science 62 (2007) 4760–4769.

[19] M. Spinola, A. Keimer, D. Segets, G. Leugering, L. Pflug, Model-based optimization of ripening processes with feedback modules, Chemical Engineering & Technology 43 (2020) 896–903.

[20] J. Maußner, H. Freund, Optimization under uncertainty in chemical engineering: Comparative evaluation of unscented transformation methods and cubature rules, Chemical Engineering Science 183 (2018) 329–345.

[21] A. L. Soyster, Convex programming with set-inclusive constraints and applications to inexact linear programming, Operations research 21 (1973) 1154–1157.

[22] A. Ben-tal, A. Nemirovski, Robust solutions of linear programming problems contaminated with uncertain data, Mathematical Programming 88 (2000) 411–424.

[23] A. Ben-Tal, D. den Hertog, J.-P. Vial, Deriving robust counterparts of nonlinear uncertain inequalities, Mathematical Programming 149 (2012).

[24] B. L. Gorissen, İhsan Yanıkoğlu, D. den Hertog, A practical guide to robust optimization, Omega 53 (2015) 124 – 137.

[25] D. Bertsimas, M. Sim, Robust discrete optimization and network flows, Mathematical programming 98 (2003) 49–71.

[26] A. Ben-Tal, A. Nemirovski, Robust convex optimization, Mathematics of operations research 23 (1998) 769–805.

[27] D. Bertsimas, O. Nohadani, K. M. Teo, Nonconvex robust optimization for problems with constraints, INFORMS journal on computing 22 (2010) 44–58.

[28] M. Kuchlbauer, F. Liers, M. Stingl, An adaptive bundle method for nonlinear robust optimization, 2020.

[29] M. Menickelly, S. Wild, Derivative-free robust optimization by outer approximations, Mathematical Programming 179 (2018).

[30] R. Reemtsen, Some outer approximation methods for semi-infinite optimization problems, Journal of Computational and Applied Mathematics 53 (1994) 87 – 108.

[31] S. Leyffer, M. Menickelly, T. Munson, C. Vanaret, S. M. Wild, A survey of nonlinear robust optimization, INFOR: Information Systems and Operational Research 58 (2020) 342–373.

[32] I. Sungur, F. Ordóñez, M. Dessouky, A robust optimization approach for the capacitated vehicle routing problem with demand uncertainty, IIE Transactions 40 (2008) 509–523.

[33] N. Remli, M. Rekik, A robust winner determination problem for combinatorial transportation auctions under uncertain shipment volumes, Transportation Research Part C: Emerging Technologies 35 (2013) 204 – 217.

[34] D. Aßmann, F. Liers, M. Stingl, Decomposable robust two-stage

optimization: An application to gas network operations under uncertainty, Networks 74 (2019) 40–61.
[35] K.-M. Aigner, J.-P. Clarner, F. Liers, A. Martin, Robust Approximation of Chance Constrained DC Optimal Power Flow under Decision-Dependent Uncertainty, 2020.
[36] A. Mersmann, Crystallization technology handbook, CRC press, 2001.
[37] M. Haderlein, D. Segets, M. Gröschel, L. Pflug, G. Leugering, W. Peukert, Fimor: An efficient simulation for zno quantum dot ripening applied to the optimization of nanoparticle synthesis, Chemical Engineering Journal 260 (2015) 706–715.
[38] T. Akdas, M. Haderlein, J. Walter, B. A. Zubiri, E. Spiecker, W. Peukert, Continuous synthesis of cuins 2 quantum dots, RSC advances 7 (2017) 10057–10063.
[39] A. Keimer, L. Pflug, Existence, uniqueness and regularity results on nonlocal balance laws, Journal of Differential Equations 263 (2017) 4023–4069.
[40] L. Pflug, T. Schikarski, A. Keimer, W. Peukert, M. Stingl, emom: Exact method of moments—nucleation and size dependent growth of nanoparticles, Computers & Chemical Engineering 136 (2020) 106775.
[41] L. Kiss, J. Söderlund, G. Niklasson, C. Granqvist, New approach to the origin of lognormal size distributions of nanoparticles, Nanotechnology 10 (1999) 25.
[42] D. Segets, C. Lutz, K. Yamamoto, S. Komada, S. Süß, Y. Mori, W. Peukert, Classification of zinc sulfide quantum dots by size: insights into the particle surface–solvent interaction of colloids, The Journal of Physical Chemistry C 119 (2015) 4009–4022.
[43] J. Van Embden, J. E. Sader, M. Davidson, P. Mulvaney, Evolution of colloidal nanocrystals: theory and modeling of their nucleation and growth, The Journal of Physical Chemistry C 113 (2009) 16342–16355.
[44] C. Forbes, M. Evans, N. Hastings, B. Peacock, Statistical distributions, John Wiley & Sons, 2011.
[45] J. Dirksen, T. Ring, Fundamentals of crystallization: kinetic effects on particle size distributions and morphology, Chemical Engineering Science 46 (1991) 2389–2427.
[46] N. T. Thanh, N. Maclean, S. Mahiddine, Mechanisms of nucleation and growth of nanoparticles in solution, Chemical reviews 114 (2014) 7610–7630.
[47] S. Süß, C. Metzger, C. Damm, D. Segets, W. Peukert, Quantitative evaluation of nanoparticle classification by size-exclusion chromatography, Powder technology 339 (2018) 264–272.
[48] B. Kowalczyk, I. Lagzi, B. A. Grzybowski, Nanoseparations: Strategies for size and/or shape-selective purification of nanoparticles, Current Opinion in Colloid & Interface Science 16 (2011) 135–148.
[49] S. J. Wright, Primal-dual interior-point methods, SIAM, 1997.
[50] J. Nocedal, S. J. Wright, Numerical Optimization, Springer, New York, NY, USA, second edition, 2006.
[51] A. Wächter, L. T. Biegler, On the implementation of an interior-point filter line-search algorithm for large-scale nonlinear programming, Mathematical programming 106 (2006) 25–57.
[52] A. S. Drud, Conopt—a large-scale grg code, ORSA Journal on computing 6 (1994) 207–216.
[53] MATLAB, 9.5.0.944444 (R2018b), The MathWorks Inc., Natick, Massachusetts, 2018.
[54] E. M. Chan, C. Xu, A. W. Mao, G. Han, J. S. Owen, B. E. Cohen, D. J. Milliron, Reproducible, high-throughput synthesis of colloidal nanocrystals for optimization in multidimensional parameter space, Nano Letters 10 (2010) 1874–1885.
[55] H.-C. Schwarzer, W. Peukert, Combined experimental/numerical study on the precipitation of nanoparticles, AIChE Journal 50 (2004) 3234–3247.
[56] T. Milek, R. W. Kirschbaum, M. S. v. Gernler, C. Lübbert, D. Segets, T. Drewello, W. Peukert, D. Zahn, On the mechanism of zn4o-acetate precursors ripening to zno: How dimerization is promoted by hydroxide incorporation, The Journal of chemical physics 143 (2015) 064501.
[57] L. Spanhel, Colloidal zno nanostructures and functional coatings: A survey, Journal of sol-gel science and technology 39 (2006) 7–24.
[58] D. Segets, M. A. Hartig, J. Gradl, W. Peukert, A population balance model of quantum dot formation: Oriented growth and ripening of zno, Chemical engineering science 70 (2012) 4–13.